Compact modeling of nonlinear distortion in analog communication circuits

Piet Wambacq, Petr Dobrovolný, Stéphane Donnay, Marc Engels, Ivo Bolsens
IMEC, Heverlee, Belgium
e-mail: wambacq@imec.be

Abstract

The design of analog front-ends of digital telecommunication transceivers requires simulations at the architectural level. The nonlinear nature of the analog front-end blocks is a complication for their modeling at the architectural level, especially when the nonlinear behavior is frequency dependent. This paper describes a method to derive a bottom-up model of nonlinear analog continuous-time circuits used in communication systems. The models take into account frequency dependence of the nonlinear behavior, making them suitable for wideband applications. Such model consists of a block diagram that corresponds to the most important contributions to the second- and third-order Volterra kernels of the output quantity (voltage or current) of a circuit. The examples in this paper, a high-level model of a CMOS low-noise amplifier and an active lowpass filter, demonstrate that the generated models can be efficiently evaluated in high-level dataflow-type simulations of mixed-signal front-ends and that they yield insight in the nonlinear behavior of the analog front-end blocks.

1. Introduction

The strong pressure for miniaturization, low power consumption and high flexibility of the front-ends of digital telecom transceivers, necessitates a study of front-ends at the architectural level. High-level simulations are an important support for such study. For these simulations, which typically combine analog parts with digital parts, commercial tools already exist, such as ADS from Hewlett-Packard [1] and SPW from Cadence [2]. Alternatively, system-level designers also use general programming languages such as C++ (e.g. see OCAPI [3]) or mathematical packages such as MATLAB [4] to perform such simulations. In these cases, the simulations are typically dataflow-based, not only for the digital blocks but also for the front-end blocks.

Although several commercial simulators contain a library with high-level models of analog blocks that can be co-simulated with the digital blocks, these models are often too general, taking into account the nominal behavior only. This leads to large inaccuracies for the simulations and, consequently, to wrong conclusions at the system level. The difficulty in modeling analog blocks at the system level is that, while the first-order, linear behavior is relatively easy to model, the nonlinear behavior requires a careful study and even advanced mathematical methods. Moreover, this nonlinear behavior can depend on frequency. This dependence is important in wideband applications. For example, in an upstream cable modem according to the MCNS standard [5], the head-end receives a frequency band between 5MHz and 42 MHz, which is almost a complete frequency decade. The nonlinear behavior of the analog front-end blocks is often not constant over such wide band. For such wideband applications the modeling method described below is a useful modeling assistant to generate high-level models for mixed-signal system-level simulations.

The signal path in the analog front-end of a communication circuit behaves in a weakly nonlinear way under normal operation. For the modeling of weakly nonlinear behavior including frequency dependence, the Fourier transforms of Volterra kernels can be used [6,7]. The first-order kernel transform describes the linear behavior of the circuit. The second-order and third-order kernel transforms, which are functions of two and three frequency variables, respectively, describe the second- and third-order nonlinear behavior. The discussion here is limited to second- and third-order nonlinear behavior only. This is a reasonable assumption in most practical cases, although the approach described here is valid as well for nonlinear behavior of order higher than three.

Whereas up till now the use of Volterra series was mainly limited to the computation at the circuit level with single-tone or two-tone excitation, the method described here uses Volterra theory to generate high-level models that can be used in conjunction with digitally modulated signals. Such signals are often difficult to approximate with a small number of sinusoidal signals. The modeling approach first computes the multidimensional Fourier transforms of second- and third-order Volterra kernels of the output of interest. These kernel transforms contain many contributions, namely one for each second- or third-order coefficient of the power series description of the different nonlinearities in the circuit. Next the approach determines the contributions that are dominant (up to a user-definable error). This method is an extension to a wideband multitone excitation of the algorithm described in [7] that only holds for a single-tone excitation. A translation of the dominant contributions into a block diagram yields the final model.

The high-level modeling of two example circuits, a low-noise amplifier and an active filter that both belong to an upstream cable modem receiver front-end, illustrates that usually few contributions dominate. This leads to compact high-levels and, moreover, a knowledge of the dominant contributions yields insight in the nonlinear circuit behavior.

The structure of the paper is as follows. Section 2 reviews the power series description of nonlinearities. Section 3 discusses the block diagram representation of nonlinear circuits. Section 4 describes the simplification of these diagrams. Section 5 contains the examples. The conclusions of the paper are formulated in Section 6.

2. Description of nonlinearities

Nonlinearities in analog circuits can be represented in admittance form, i.e. by a (nonlinear) model equation that describes a current as a function of one or more controlling voltages. For example, the AC drain current i_d of a MOS transistor can be written as a Taylor series with the controlling voltages v_{gs}, v_{ds} and v_{sb} [7]:

$$\begin{aligned} i_d &= gm \cdot v_{gs} + K2_{gm} v_{gs}^2 + K3_{gm} v_{gs}^3 + go \cdot v_{ds} + K2_{go} v_{ds}^2 \\ &+ K3_{go} v_{ds}^3 - gmb \cdot v_{sb} - K2_{gmb} v_{sb}^2 - K3_{gmb} v_{sb}^3 + K2_{gm\&go} v_{gs} v_{ds} \\ &+ K3_{gm\&2go} v_{gs} v_{ds}^2 + K3_{2gm\&go} v_{gs}^2 v_{ds} + K2_{gm\&gmb} v_{gs} v_{sb} \\ &+ K3_{gm\&2gmb} v_{gs} v_{sb}^2 + K3_{2gm\&gmb} v_{gs}^2 v_{sb} + K2_{gmb\&go} v_{sb} v_{ds} \\ &+ K3_{gmb\&2go} v_{sb} v_{ds}^2 + K3_{2gmb\&go} v_{sb}^2 v_{ds} + K3_{gm\&gmb\&go} v_{gs} v_{ds} v_{sb} + \mathrm{K} \end{aligned} \quad (1)$$

in which the coefficients *K2* and *K3*, referred to as second- and third-order nonlinearity coefficients, are proportional to the second- and third-order derivative of the drain current. Coefficients that correspond to derivatives with respect to one voltage, are called one-dimensional nonlinearity coefficients. The ones proportional to cross-derivatives, such as $K2_{gm\&go}$ and $K3_{gm\&gmb\&go}$ are two-dimensional and three-dimensional nonlinearity coefficients, respectively. Nonlinear capacitors can be described by a one-dimensional Taylor series that expresses the charge upon the capacitor as a function of the voltage over the capacitor. The AC current through the capacitor is simply found by differentiating this charge with respect to time.

3. Block diagram representation of Volterra kernels

A block diagram for a Volterra kernel of a voltage or current in a nonlinear analog circuit can be constructed by an adoption of the technique described in [6]. To understand this construction, consider a one-dimensional second- or third-order nonlinearity coefficient of a nonlinear admittance. A second-order nonlinearity squares the voltage over its controlling terminals, then multiplies the result with its second-order nonlinearity coefficient to produce a second-order "nonlinear" current. This current propagates to the output. When the second-order response is to be computed, then only the linear propagation of this current to the output must be considered. The effect of other nonlinearities on this current can indeed be neglected, since this yields nonlinear behavior of order higher than two. This reasoning holds for all second-order nonlinearity coefficients in the circuit. Hence, the total second-order output is the sum of the contributions of all second-order nonlinearity coefficients. As shown in Figure 1, each contribution corresponds to one path in the block diagram representation.

A block diagram representation of a second-order Volterra kernel contains three different types of paths, corresponding to one-dimensional second-order nonlinearity coefficients $K2_{g..}$, two-dimensional coefficients $K2_{ga\&gb..}$ and to coefficients $K2_{C..}$ that correspond to nonlinear capacitors. The transfer function from the input to the voltage that controls the nonlinearity is denoted by **H**… Transfer functions from a second-order current – which flows from the positive terminal of a nonlinearity to its negative terminal – to the output of the circuit are denoted by **TF**…, and they are computed in the linearized circuit.

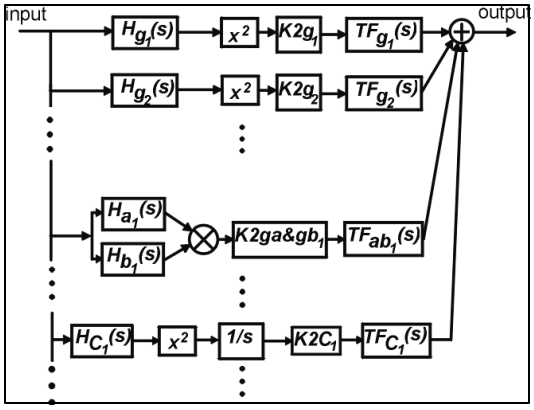

Fig. 1: block diagram for the computation of the second-order nonlinear behavior of a nonlinear circuit.

Each path consists of a second-order nonlinearity coefficient, linear transfer functions and a static nonlinearity. For a one-dimensional nonlinearity this nonlinearity is a squarer, while for a two-dimensional nonlinearity this is a multiplier that takes the product of the two parallel paths that correspond to the two controlling voltages. With a block diagram such as in Fig. 1, the output of the circuit due to second-order nonlinear behavior can be computed for any input excitation, provided that this excitation is not too large such that the assumption of weakly nonlinear behavior is not violated.

The construction of a block diagram for third-order nonlinear behavior caused by third-order nonlinearity coefficients (see Figure 2) proceeds in a similar way as second-order behavior caused by second-order nonlinearities. On the other hand, as shown in Figure 3, second-order nonlinearities produce a third-order nonlinear response by combining

at their controlling terminals a second-order signal with a first-order signal to produce a third-order "nonlinear" current. A block diagram for the second-order signal is similar to the one of Figure 1. The propagation of the third-order nonlinear current through the linearized circuit yields the contribution of the second-order coefficient to the overall third-order output signal. The total third-order kernel is then modeled as the parallel connection of different paths as the ones shown in Fig. 2 and 3. Clearly, block diagrams that describe third-order nonlinear behavior, contain only scale factors, linear transfer functions and static nonlinearities, just as in the second-order case.

Fig. 2: path from the input to the output of a weakly nonlinear circuit corresponding to the contribution of a one-dimensional third-order coefficient $K3_{g1}$ to the overall third-order nonlinear behavior.

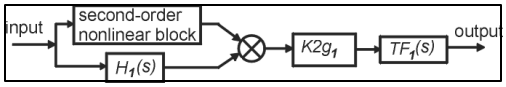

Fig. 3: path from the input to the output of a weakly nonlinear circuit corresponding to the contribution of a one-dimensional second-order coefficient $K2_{g1}$ to the overall third-order nonlinear behavior.

4. Simplification of the block diagrams

In a circuit of practical size the block diagrams for the second- and third-order nonlinear behavior consist of many parallel paths. This is already clear from the large number of nonlinearity coefficients that is required to describe the drain current of one MOS transistor (see equation (1)). The use of such bulky diagram for system-level simulations is not practical.

Fortunately, in most practical circuits many nonlinearity coefficients give a negligible contribution to the overall second- or third-order nonlinear behavior. This is exploited in an algorithm that eliminates all negligible contributions up to a user-definable error on the magnitude and phase of the kernel transforms in a given frequency band of interest. The algorithm is an extension to multiple dimensions of the method described in [7] to determine the most important contributions to the second- and third-order harmonics. Indeed, digital telecom signals require evaluations of the kernels for all frequency arguments being different. In addition, negative values for the frequency arguments must be considered as well. Two properties of kernel transforms are used to reduce the number of evaluations: the symmetry of kernel transforms [6] and the property that a change of the sign of one of the frequency arguments yields the complex conjugate of the kernel transform.

This approximation procedure uses transfer functions and nonlinearity coefficients that are precomputed with a circuit simulator, in this case HSPICE. The nonlinearity coefficients are computed by numerical differentiation on data from DC analyses.

The running time limit of this approach for the construction of a block diagram that approximates the kth-order nonlinear behavior is $O(n^4.f + M.\log(M).f^k)$, where n is the number of nodes in the circuit, f is the number of different frequencies that are considered and M is the number of nonlinearity coefficients of order $2, \ldots, k$. This running time limit shows that high-order behavior (i.e. higher than three) yields excessive computations if the frequency resolution is very high.

5. Examples

As an illustration a high-level model is constructed for the amplifier and the active anti-alias filter of the integrated receiver front-end architecture (see Fig. 4) for an upstream cable modem in the MCNS standard. Both circuits are designed in a digital 0.35µm CMOS process.

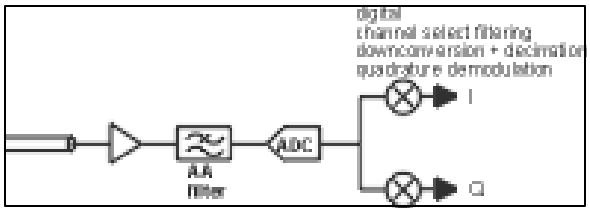

Fig. 4: maximally digital receiver front-end architecture for upstream cable modem applications.

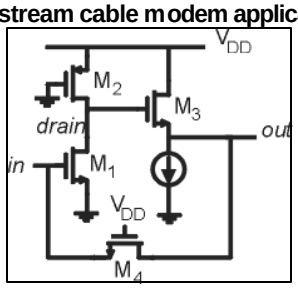

Fig. 5: simplified schematic of a CMOS amplifier for upstream cable modem applications. The gain is 12, the input impedance is 75Ω.

For the amplifier we limit the discussion to third-order nonlinear behavior, since this requires more computations than the second-order behavior. The third-order Volterra kernel transform of the amplifier's output voltage is a function of three frequencies f_1, f_2 and f_3, and it has 37 contributions each corresponding to a second- or third-order nonlinearity coefficient. The input signal has a bandwidth from 5 MHz to 42 MHz, which is also the band of interest at the output of the amplifier. The elimination procedure

evaluates the kernel transform and its contributions for combinations of $\pm f_1$, $\pm f_2$ and $\pm f_3$ with f_1, f_2 and f_3 between DC and 42 MHz.

The third-order kernel can be approximated well by one single contribution, namely the one from $K2_{go2}$. This is the second-order nonlinearity of the output conductance of transistor M_2, which operates in the triode region. This nonlinearity is determined by the drain-source voltage of M_2. It is not a surprise that the largest contribution comes from M_2: nonlinearities that are controlled by voltages that experience high swings, in general yield a large contribution. In the circuit of Fig. 5 there is a voltage gain between node "in" and node "drain", such that the voltage swing at the latter node is quite high. The main contributions to the third-order kernel are best visualized by a 2-D plot (see Fig. 6) from which the dominance of the contribution of $K2_{go2}$ is obvious.

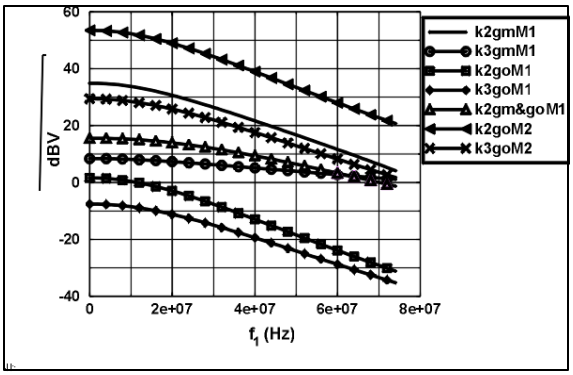

Fig. 6: third-order kernel transform of the amplifier output voltage, and its most important contributions, evaluated for f_1=f_3 and f_2 fixed at -42 MHz. The input amplitude is taken equal to 1V as a reference, yielding artificially large intermodulation products.

Having the most important contribution, we now construct an approximate simulation model for the third-order nonlinear behavior in the form of a block diagram. It is clear from Fig. 3 that the contribution of $K2_{goM2}$ depends on the second-order kernel transform of the voltage that determines this nonlinearity. This second-order kernel in turn consists of several contributions. The approximation procedure finds that the main contribution to this kernel again comes from $K2_{goM2}$. The result is shown in Fig. 7.

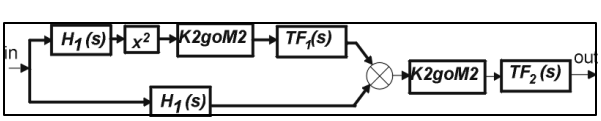

Fig. 7: approximate high-level model for the third-order nonlinear behavior of the LNA of Fig. 5.

The final block diagram, shown in Fig. 7, contains three transfer functions: $H_1(s)$ is the transfer function from the input voltage source (with an output impedance of 75O) to the voltage of node "drain", which is the controlling voltage of the nonlinearity $K2_{goM2}$. Further, $TF_1(s)$ and $TF_2(s)$ denote the transfer functions from the nonlinear current source that corresponds to $K2_{goM2}$, to the voltage at the nodes "drain" and "out", respectively. This nonlinear current source flows from the node "drain" to the AC ground.

Although the approximate model is compact, the accuracy is fairly good: compared to the exact value of the third-order kernel evaluated at all frequency combinations in the band of interest, the maximum error on the magnitude of the approximate model is 13%.

The need to consider the frequency dependence of the nonlinear behavior is evidenced by a system-level simulation in MATLAB on the receiver front-end of Fig. 4. In this simulation, the amplifier excitation consists of different channels between 5 and 42 MHz. Each channel has a 3.2 MHz bandwidth and a power of 6dBmV. The amplifier is modeled by its linear transfer function and an approximation of the second-order and third-order (see Fig. 7) kernel transforms. In this amplifer model, outputs of blocks that represent transfer functions are computed in the frequency domain, while outputs of static nonlinearities are computed in the time domain. The anti-alias filter is modeled for this simulation by its linear transfer function only. For the ADC only the sampling operation and the quantization are modeled.

Nonlinear behavior of the amplifier causes channel interference at the amplifier output. As shown in Fig. 8, neglecting the frequency dependence of the nonlinear behavior yields a signal-to-distortion ratio in one channel that is up to 6.5 dB smaller than if the frequency dependence is taken into account. This illustrates the importance of the frequency dependence in wideband applications.

For circuits that are larger than the amplifier of Fig. 5, the modeling approach described in this paper can still generate fairly compact approximate high-level models for the frequency-dependent nonlinear behavior. To illustrate this, we realize the anti-alias filter in the front-end as a fully differential 3rd-order elliptic gm-C filter (see Fig. 9), and we derive an approximate model for the second-order nonlinear behavior. Due to mismatches this second-order nonlinear behavior is not completely suppressed. The –3dB frequency of this filter is 47 MHz. The transconductor that is used in this filter is shown in Fig. 10.

The approximation procedure finds that the main contributions to the second-order nonlinear behavior come from the nonlinearity of the transconductance of M1 and M2 in the transconductor with label X4 in Fig. 9. As seen in Fig. 11, the total value of the intermodulation product is smaller than the largest contributions. If there would be no mismatches, then these contributions are two-by-two opposite and with equal magnitude, such that the total second-order kernel is zero. If the six contributions shown in Fig. 11 are taken into account for the approximation of the

second-order kernel transform, then the maximum error on the magnitude of the second-order kernel, evaluated over the complete passband of the filter, is only 1.1 dB. The resulting high-level model is still fairly compact with twelve transfer functions, six squarers and six scale factors.

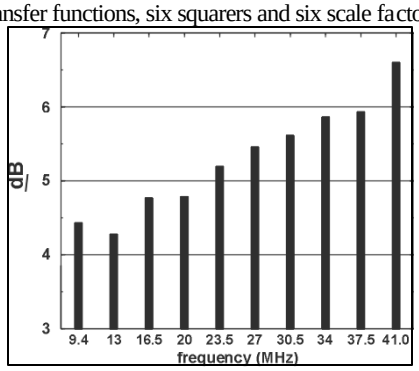

Fig. 8: difference in dB in signal-to-distortion ratio obtained from high-level simulations with and without taking into account frequency dependence of the nonlinear models. The x-axis indicates the center frequency of the channels.

The CPU time for the computation of both second- and third-order responses of the filter, followed by the approximation phase is 10 seconds on a 400 MHz Intel Pentium II processor with a Linux operating system.

6. Conclusions

Modeling and understanding nonlinear behavior of analog integrated communication circuits is not straightforward, since in a practical circuit many nonlinearities contribute to the overall nonlinear behavior. Moreover, these contributions depend on frequency. This paper has described an approach that determines the most important contributions to second- and third-order nonlinear behavior of the circuit with the inclusion of frequency dependence. A translation of these dominant contributions into a block diagram yields high-level models that are useful for high-level simulations of front-end architectures. The examples in this paper show that these models are very compact for practical circuits, even when parasitic effects such as mismatches are taken into account. The models contain a small number of linear transfer functions, static nonlinearities and scale factors. In this way, the approach described in this paper is useful to construct bottom-up models that yield efficient high-level simulations, and to obtain insight in the nonlinear operation of analog integrated communications circuits.

References

[1] ADS,Hewlett-Packard, www.tmo.hp.com/tmo/hpeesof
[2] SPW,Cadence, www.cadence.com/alta
[3] P. Schaumont et al., "A programming environment for the design of complex high speed ASICs", *Proc. DAC*, pp. 315-320, 1998.
[4] Matlab, Math Works, http://www.mathworks.com
[5] MCNS-DOCSIS, CableLabs' Website: www.cablemodem.com
[6] M. Schetzen, *"The Volterra and Wiener theories of nonlinear systems,"* J. Wiley and Sons, 1980.
[7] P. Wambacq and W. Sansen, *"Distortion analysis of analog integrated circuits,"* Kluwer Academic Publishers, 1998.

Acknowledgements

This work has been funded by the Flemish IWT-sponsored IT-ISIS project and by the ESPRIT project SALOMON.

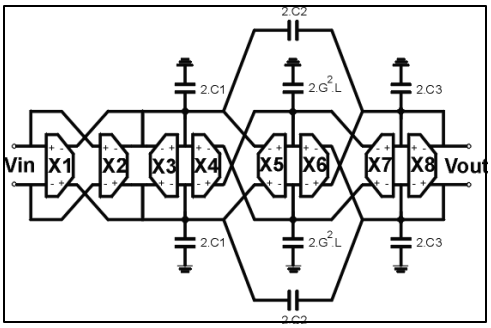

Fig. 9: 3rd-order elliptic lowpass filter.

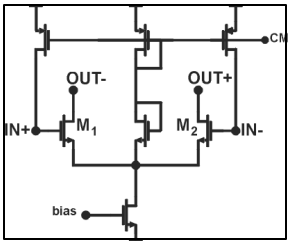

Fig. 10: transconductor used in the lowpass filter.

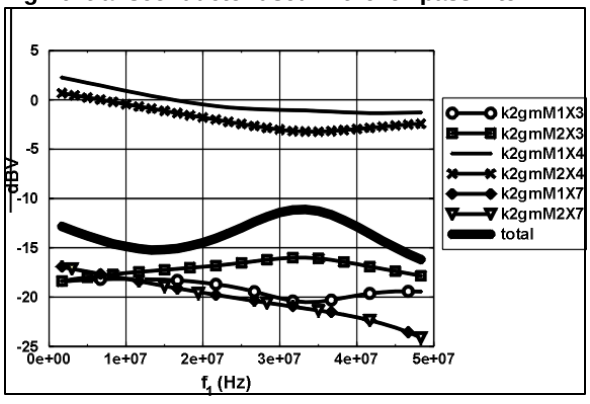

Fig. 11: most important contributions to the 2nd-order intermodulation product at $|f_1-f_2|$ at the output of the filter of Fig. 9 with f_2=10 MHz. The input amplitude is taken equal to 1V as a reference.